Quantitative Diffusion-Weighted Magnetic Resonance Imaging of Ovarian Masses

Ovaryen Kitlelerin Görüntülenmesinde Kantitatif Difüzyon-Ağırlıklı Manyetik Rezonans

Ercan İNCİ, MD,[a]
Özgür KILIÇKESMEZ, MD,[b]
Bengi GÜRSES, MD,[b]
Neslihan TAŞDELEN, MD,[b]
Sibel AYDIN, MD,[a]
Tan CİMİLLİ, MD,[a]
Nevzat GÜRMEN, MD[b]

[a]Department of Radiology, Yeditepe University Medical Faculty
[b]Department of Radiology, İstanbul Bakırköy Dr. Sadi Konuk Training and Research Hospital, İstanbul

Geliş Tarihi/*Received:* 21.10.2009
Kabul Tarihi/*Accepted:* 03.12.2010

Yazışma Adresi/*Correspondence:*
Ercan İNCİ, MD
Bakırköy Dr. Sadi Konuk Training and Research Hospital, Department of Radiology, İstanbul, TÜRKİYE/TURKEY
ercan@inci.com

ABSTRACT Objective: The purposes of this study were to calculate the apparent diffusion coefficient (ADC) values of ovarian masses and to determine whether they were different in benign and malignant masses. **Material and Methods**: A total of 51 patients with 59 benign and malignant ovarian masses were enrolled in the study. Diffusion-weighted magnetic resonance imaging (DW MRI) was performed with b factors of 0, 500 and 1000 s/mm^2. **Results:** The mean ADC value of the ovarian masses were 3.00 ± 0.26 x 10^{-3} mm^2/s for functional (follicle) cysts, 1.30 ± 0.47 x 10^{-3} mm^2/s for hemorrhagic cysts, 1.32 ± 0.34 x 10^{-3} mm^2/s for endometriomas, 1.03 ± 0.15 x 10^{-3} mm^2/s for dermoid cysts, 2.79 ± 0.25 x 10^{-3} mm^2/s for cystadenomas, and 1.29 ± 0.31 x 10^{-3} mm^2/s for carcinomas. There were significant differences in ADC values for cystadenomas and carcinomas ($p< 0.031$) as well as for dermoid cysts and endometriomas-hemorrhagic cysts ($p< 0.05$). The ADC values of functional cysts-cystadenomas did not differ. **Conclusion:** The ADC values of benign and malignant ovarian lesions overlap considerably. The DWI does not provide additional information to conventional sequences for discrimination of benign and malignant masses.

Key Words: Magnetic resonance imaging; diffusion magnetic resonance imaging; ovarian neoplasms

ÖZET Amaç: Bu çalışmanın amacı, ovaryen kitlelerin görünür difüzyon katsayısı (ADC) değerlerini hesaplamak ve bu değerlerin kitlelerin selim ve habis lezyonlarda farklı olup olmadığını değerlendirmektir. **Gereç ve Yöntemler:** Toplam 51 hastaya ait 59 selim ve habis tümör çalışmada değerlendirilmiştir. Difüzyon ağırlıklı magnetik rezonans görüntüleme (DA-MRG), 0, 500 ve 1000 s/mm^2 b faktörleri ile gerçekleştirilmiştir. **Bulgular:** Ovaryen kitlelere ait ortalama ADC değerleri sırasıyla, folikül kistleri için 30 ± 0.47 x 10^{-3} mm^2/s, endometriomalar için 1.32 ± 0.34 x 10^{-3} mm^2/s, dermoid kistler için 1.03 ± 0.15 x 10^{-3} mm^2/s, kist adenomlar için 2.79 ± 0.25 x 10^{-3} mm^2/s ve karsinomalar için 1.29 ± 0.31 x 10^{-3} mm^2/s bulundu. Kist adenomlar ve karsinomaların ADC değerlerinde ($p< 0.031$) dermoid kist ve endometrioma-hemorajik kistlerde olduğu gibi anlamlı farklılık mevcuttu ($p< 0.05$). Fonksiyonel kistler ile kistadenomların ADC değerleri farklı bulunmadı. **Sonuç:** Selim ve habis tümörlerin ADC değerleri anlamlı bir şekilde örtüşme bulundu. DA-MRG' nin, selim ve habis tümörlerin ayrımında kullanılan klasik sekans değerlerine ilave katkı sağlamamıştır.

Anahtar Kelimeler: Manyetik rezonans görüntüleme; difüzyon manyetik rezonans görüntüleme; over tümörleri

Turkiye Klinikleri J Med Sci 2011;31(1):86-92

Adnexal masses are frequently encountered in the medical practice.[1,2] Determination of a cut-off level for malignancy of an adnexal mass is critical and is mainly based on the appearance of the mass on imaging. This cut-off level would determine the need for surgery, referral to a surgeon, and the urgency for surgery. Ovarian cancer is a leading cause of

doi:10.5336/medsci.2009-15860

death from gynecologic malignancies and the fifth most common cause of cancer deaths in women. Most patients present in advanced stages of the disease due to the silent clinical course.[3-5]

Ultrasound is the primary modality used for detection and characterization of adnexal masses and remains as the study of choice because it is relatively inexpensive, noninvasive, and widely available. The identification of ovarian masses depends on tissue characterization based on magnetic resonance (MR) properties. The superior contrast resolution of MR makes it valuable in characterizing a sonographically indeterminate adnexal mass.[6] Furthermore, diffusion weighted imaging (DWI) has emerged as a diagnostic tool for the evaluation of oncologic and inflammatory diseases. For two decades, DWI has been applied to the evaluation of intracranial diseases; the development of fast imaging such as echo planar imaging and parallel imaging techniques and recently new software enabled to overcome the difficulties and restrictions of abdominal DWI.[7,8] The purpose of this study was to evaluate the feasibility of DWI for discrimination of benign and malignant ovarian masses.

MATERIAL AND METHODS

PATIENT POPULATION

This retrospective study was conducted in a single institution. During a period of 12 months, a total of 51 women (mean age of 53 years) with 59 known benign and malignant ovarian lesions previously diagnosed with ultrasound and MRI consisting of functional cysts (12 cases), hemorrhagic cysts (seven cases), dermoid cysts (nine cases), endometriomas (11 cases), cystadenomas (nine cases, seven being serous cystadenomas and two being mucinous cystadenomas), and carcinomas (11 cases, six being serous cystadenocarcinomas, three being Krukenberg tumors, one being mucinous cystadenocarcinoma, and one being granulosa cell tumor) were included in the study.

The research protocol was approved by the ethics committee. Written consent was obtained from all patients prior to commencement of the study.

The diagnosis of hemorrhagic cysts was based on imaging findings and detection of resolution on serial imaging. The diagnoses of dermoid cysts, cystadenomas and carcinomas were based on histopathological examinations. Endometriotic cysts were diagnosed referring to imaging findings (multiplicity, T2 shading and clinical findings) in five cases and the others were diagnosed histopathologically.

MR TECHNIQUE

The MR imaging was performed on a 1.5 T body scanner (Avanto; Siemens, Erlangen, Germany) with a 33 mT/m maximum gradient capability using an eight-channel body coil phased-array for signal repetition. Technical parameters of the sequences used for pelvic MRI were as follows:

1) ***Axial, turbo spin-echo T2-weighted sequence*** repetition time [TR], 4320 ms; echo time [TE], 87 ms; flip angle [FA], 150°; matrix, 320 x 240; slice numbers, 30; slice thickness= 6.5 mm; interslice gap, 30%; field of view [FOV], 50 cm; averages, 2; acquisition time, 2.24 s; bandwidth, 130 Hz/Px.

2) ***Axial fat-saturated 3D gradient-echo T1-weighted MR sequence (VIBE)*** *TR,* 5.32 ms; *TE,* 2.53 ms; *FA,* 10°; matrix, 256 x 166; slice numbers, 80; slice thickness= 3.6 mm; interslice gap, 20%; FOV, 45 cm; averages, 1; acquisition time, 0:16 s; bandwidth, 300Hz/Px, PAT mode, generalized autocalibrating partially parallel acquisitions [GRAPPA]; PAT factor, 2.

3) ***Axial, turbo spin-echo T1-weighted sequence*** *TR,* 536 ms; *TE,* 11 ms; *FA,* 150°; matrix, FOV, 50 cm; averages, 1; acquisition time, 1.33 s; bandwidth, 130 Hz/Px.

4) ***Sagittal, turbo spin-echo T2-weighted sequence*** *TR,* 5030 ms; *TE,* 101 ms; *FA,* 150°; matrix, 384 x 288; slice numbers, 24; slice thickness= 6 mm; interslice gap, 30%; FOV, 36 cm; averages, 2; acquisition time, 2,37 s; bandwidth, 130 Hz/Px.

5) ***Coronal, turbo spin-echo time sequence*** *TR,* 4980 ms; *TE,* 84 ms; *FA,* 150°; matrix, 320 x 240; slice numbers, 20; slice thickness= 7 mm; interslice gap, 30%; FOV, 37 cm; averages, 2; acquisition

time, 2.24 s; bandwidth, 220 Hz/Px; PAT mode, GRAPPA; PAT factor.

6) ***High b-value diffusion weighted single-shot spin echo echo-planar sequence*** with, chemical shift selective fat-suppression technique; TR/TE, 4900/93; matrix, 192 × 192; slice numbers, 30; slice thickness = 6 mm; interslice gap, 35%; FOV, 45 cm; averages, 5; acquisition time, approximately 3 minutes, PAT factor, 2; PAT mode, GRAPPA was performed.

Following DWI, contrast enhanced imaging was performed with axial and sagittal 3D gradient-echo T1-weighted MR sequence after administration of gadopentetate dimeglumine at a dose of 0.1 mmol/kg of body weight as a bolus injection (each breath hold lasted between 20-24 s).

IMAGE INTERPRETATION

The DWI datasets were transferred to an independent Workstation (Leonardo console, software version 2.0; Siemens) for postprocessing. The DW images were of diagnostic quality in all cases, and no cases were excluded from the study. The ADC maps were calculated and mapped by the imaging system software. To measure ADC values of the masses, a free hand ROI was defined on the T2-weighted EPI image (*b*=0), while referring to the axial T1 and T2-weighted and contrast enhanced images for verification of the lesion boundaries. The ROI was then copied to the corresponding ADC map. The ROI included all lesions in completely cystic mass lesions. The solid component was measured in mixed solid and cystic masses.

STATISTICAL ANALYSIS

All statistical analyses were performed using SPSS (Version 10.0 for Windows release, Chicago, IL, USA). The ADC values of patients were reported as the mean ± STD. The normality of distribution of the parameters was assessed using the Kolmogorov–Smirnov test. One-way ANOVA was employed to determine the differences in the ADC values by the lesion types and mean differences were attained by Tukey HSD test. A p value of less than 0.05 was considered significant.

RESULTS

The ADC values for ovarian masses underwent conventional and DW MRI examinations are summarized in Table 1. Disease groups are shown in Figure 1 (scatter plots). There was significant difference in ADC values between cystadenomas and carcinomas ($p< 0.001$) as well as between dermoid cysts and he-

TABLE 1: Comparison of the subgroups of ovarian masses.

Lesion	N	Mean ADC (mm^2/s)	Comparison[1]
Functional cyst	12	$3.00 \pm 0.26 \times 10^{-3}$	Functional cyst>Hemorrhagic cyst Functional cyst>Endometriotic cyst Functional cyst>Dermoid cyst Functional cyst>Carcinomas
Hemorrhagic cyst	7	$1.30 \pm 0.47 \times 10^{-3}$	Hemorrhagic cyst< Functional cyst Hemorrhagic cyst< Cystadenomas
Endometriotic cyst	11	$1.32 \pm 0.34 \times 10^{-3}$	Endometriotic cyst< Functional cyst Endometriotic cyst< Cystadenomas
Dermoid cyst	9	$1.03 \pm 0.15 \times 10^{-3}$	Dermoid cyst< Functional cyst Dermoid cyst< Cystadenomas
Cystadenomas	9	$2.79 \pm 0.25 \times 10^{-3}$	Cystadenomas> Hemorrhagic cyst Cystadenomas> Dermoid cyst Cystadenomas> Carcinomas Cystadenomas> Endometriotic cyst
Carcinomas	11	$1.29 \pm 0.31 \times 10^{-3}$	Carcinomas< Functional cyst Carcinomas< Cystadenomas

1p< 0.001 (post hoc Tukey HSD test).

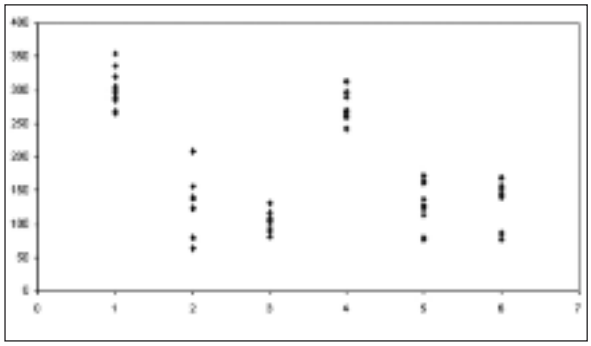

FIGURE 1: Scatter plots of the ADC values obtained in benign and malignant lesions. (1: Functional cysts, 2: Hemorrhagic cysts, 3: Dermoid cysts, 4: Cystadenomas, 5: Carcinomas, 6: Endometriomas).

morrhagic cysts-endometriomas ($p< 0.005$). The ADC values between functional cysts and cystadenomas; between hemorrhagic cysts and endometriomas; and between endometriomas-hemorrhagic cysts and carcinomas were not different (Figure 2, 3, 4).

DISCUSSION

The goal of imaging for adnexal masses is to determine malignancy and guide for treatment options. Ovarian masses with septations greater than 3 mm, mural nodularity, and papillary projections indicate a malignant ovarian neoplasm. The most significant feature is the presence of solid components within an ovarian mass. Some benign lesions and most commonly endometriomas and hemorrhagic cysts may have a similar appearance with malignant ovarian tumors.[3,9] We hypothesized if DWI was able to determine malignant lesions of the ovary.

Normal ovaries reflect high cortical signal on DW images probably because of the cellular component of cortical stroma and dense connective tissue, in contrast relatively low signal intensity in the hilum and central stroma probably related to looser vascular and connective tissue.[2] We did not calculate the normal ADC values of ovaries, because of relatively small volume, the difficulty of calculation of normal ovarian parenchyma with the avoidance of inclusion of follicles, and interference of normal menstrual cycle on the parenchyma.

The cortex of the ovary frequently contains follicles at various stages. In the preovulatory period, dominant preovulatory follicles can enlarge by

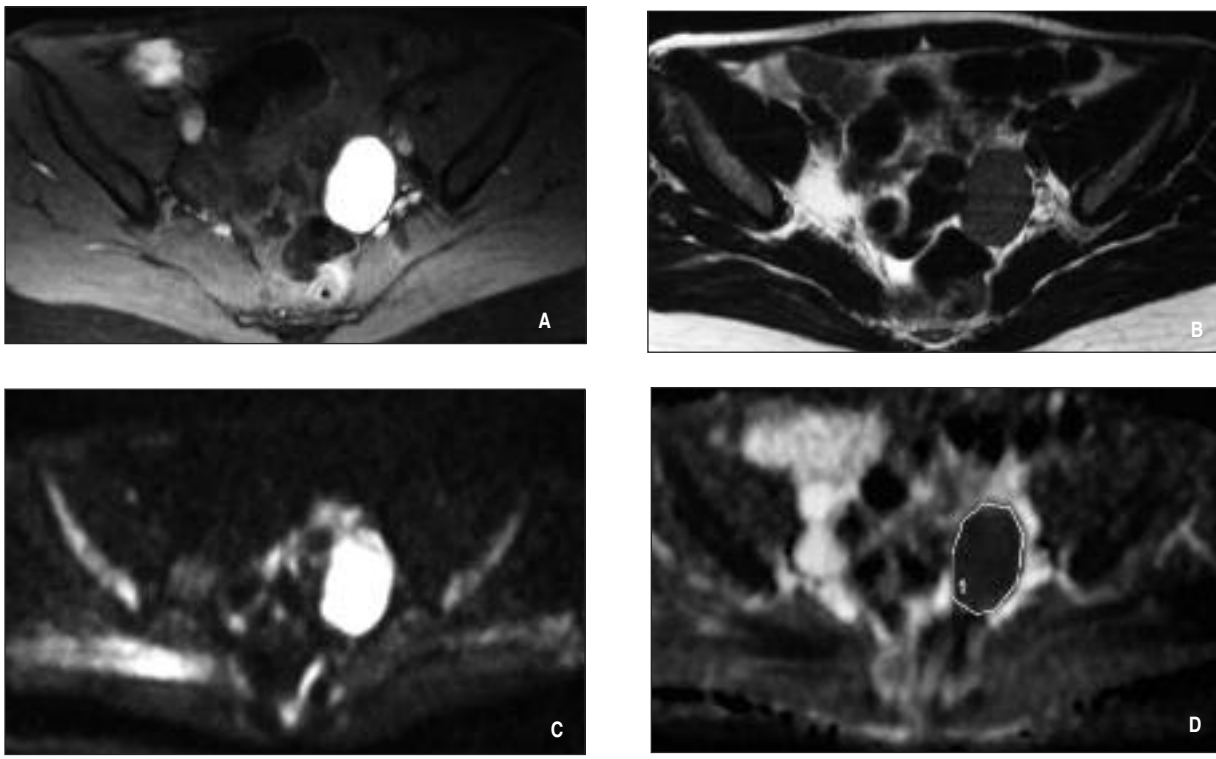

FIGURE 2: A 54-year-old woman with endometrioma. **A** Non-enhancing (not shown here) left adnexal mass shows hyperintensity on VIBE image. **B** T2-weighted image demonstrates hypointensity (shading). **C** DWI of the mass shows hyperintensity (b= 1.000 s/mm^2). **D** Apparent diffusion coefficient (ADC) was calculated. Mass on ADC image shows hypointensity (decreased diffusion). Region of interest (ROIs) was placed on the mass (ROI 1,d). ADC of the mass was 1.25 x 10^{-3} mm^2/s.

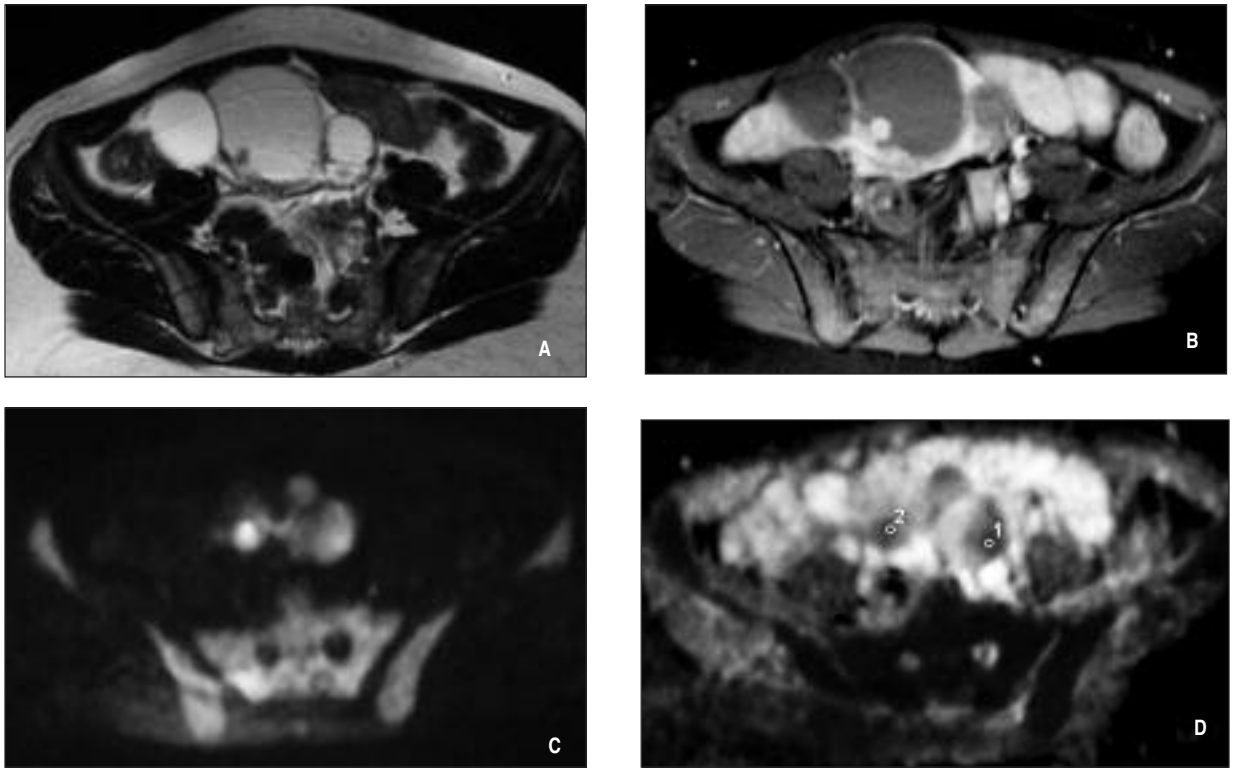

FIGURE 3: A 48-year-old woman with serous cystadenocarcinoma. **A** Complex, mixed solid and cystic pelvic mass shows hyperintensity on T2-weighted image. **B** Hypointensity of the cystic components and enhancing walls and mural nodule on the VIBE image. **C** Hyperintensity of the solid mural nodule on diffusion-weighted (b= 1.000 s/mm^2) images. **D** Apparent diffusion coefficient (ADC) was calculated. Mural nodule on ADC image shows hypointensity (decreased diffusion). Region of interest (ROIs) was placed on the solid portion (ROI 1,2d). ADC of the mass was 1.19 x 10^{-3} mm^2/s and 1.23 x 10^{-3} mm^2/s respectively.

17-25 mm.[10] When a follicle fails to involute or ovulate, a follicular cyst develops. These cysts can range from 3 to 8 cm but rarely exceed 5 cm.[11,12] Since large follicular cysts may be indistinguishable from neoplastic cysts, they should be followed up. Unlike neoplastic cysts, follicular cysts may spontaneously regress over time, usually within two menstrual cycles. In our study large functional cysts were indiscernible from serous cystadenomas both on conventional and DW MR imaging.

Hemorrhagic ovarian cysts are mostly hemorrhagic functional or corpus luteum cysts. These cysts arise when corpus luteum fails to regress. They usually have a thicker wall with a slight hyperintensity on T1-weighted images. The most frequently encountered hemorrhagic corpus luteum cysts are seen in the subacute phase and display a high signal intensity on T1-and T2-weighted images. They may be misdiagnosed as endometriomas, however, on follow-up endometriomas persist.[11,13] Additionally, endometriomas are highly hyperintense on T1-weighted images and hypointense on T2-weighted images. In this study, the ADC values of functional cysts and hemorrhagic cysts were different ($p< 0.01$). Discrimination between these masses has already been easily performed with conventional sequences. There was no statistical significance between the ADC values of endometriomas and hemorrhagic cysts.

Dermoid cysts are easily discernible from T1 hyperintense lesions such as endometrial cysts by suppression of the signal of fatty component with frequency-selective fat suppression techniques.[2,5] In the present study, these lesions showed the lowest ADC values among the ovarian masses ($p< 0.001$).

Cystadenomas had higher ADC values than carcinomas facilitating their discrimination ($p< 0.001$). In fact, these two groups may easily be differentiated with well known classical findings reported in the literature, including enhancing

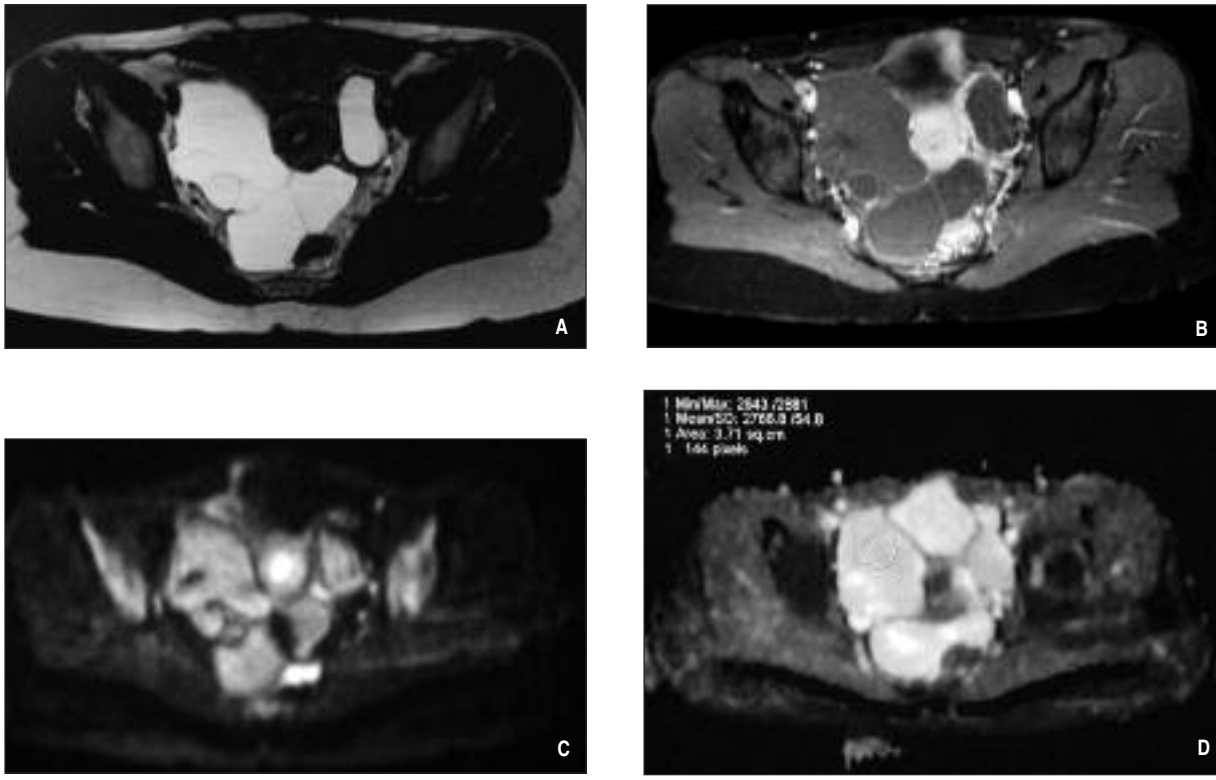

FIGURE 4: A 29-year-old woman with serous cystadenoma **A.** A multiseptated cyst in the right adnexal region shows hyperintensity on T2-weighted image. **B.** Hypointensity of the cystic components and lack of enhancement on the VIBE image. **C.** Mild hyperintensity of the cyst on diffusion-weighted (b= 1.000 s/mm^2) image (T2 shine through effect). **D.** Apparent diffusion coefficient (ADC) was calculated. Region of interest (ROI) was placed on the cyst (ROI 1,d). ADC of the cyst was 2.76 x 10^{-3} mm^2/s.

papillary projections, solid components, and thick septations.[2,3]

There are papers that are in agreement and disagreement with our data. In concordance with the present study, Moteki and Ishizaka[14] stated that endometrial cysts and malignant cystic ovarian tumors had lower ADC values than ovarian cysts and serous cystadenomas ($p< 0.03$). In another study conducted by Nakayama et al.,[15] similarly the lowest ADC values were detected from dermoid cysts and this was attributed to keratinoid substances within these masses. In a previous study performed by Katayama et al.[16] the lesions exhibiting typical watery intensity tended to have higher ADCs than those exhibiting atypical watery intensity on T1- and T2-weighted images. In addition, according to a recent study performed by Takeuchi et al.,[17] low intensity on DWI with high ADC may suggest benign lesions; however, it may be occasionally difficult to differentiate benign and malignant lesions only on the basis of DWI. The differences in ADCs, therefore, were more closely related to the signal intensity of the fluid rather than a histopathologic group; finally they concluded that ADCs of ovarian lesions were unable to discriminate benign from malignant ones.

Recent studies have shown that DW imaging plays an important role in the diagnosis and therapeutic management of patients with gynecologic malignancies. The DWI has a high sensitivity and specificity for the evaluation peritoneal dissemination as well.[18, 19] In our study DWI was able to detect all metastatic implants, in three patients with metastatic spread.

Our study has some limitations. First, the sample size was small to constitute subgroups. Second, some of the lesions we detected were diagnosed with imaging findings and follow up imaging. When endometriomas, hemorrhagic cysts and dermoid cysts demonstrating lower ADC values were

excluded by the help of conventional MRI sequences, ADC mapping may be helpful for detection of malignancy in mixed solid and cystic masses.

However, without the assistance of conventional MRI sequences, ADC values of benign and malignant lesions overlap and this can lead to misdiagnoses. In conclusion, on the basis of these findings, the DWI does not provide additional information to discriminate benign from malignant masses.

REFERENCES

1. Jeong YY, Outwater EK, Kang HK. Imaging evaluation of ovarian masses. Radiographics 2000;20(5):1445-70.
2. Outwater EK, Dunton CJ. Imaging of the ovary and adnexa: clinical issues and applications of MR imaging. Radiology 1995(1);194:1-18.
3. Mironov S, Akin O, Pandit-Taskar N, Hann LE. Ovarian cancer. Radiol Clin North Am 2007;45(1):149-66.
4. Devine C, Szklaruk J, Tamm EP. Magnetic resonance imaging in the characterization of pelvic masses. Semin Ultrasound CT MR 2005;26(3):172-204.
5. Pakkal MV, Balogun M. Imaging of ovarian cancer. Imaging 2006;18(3):20-7.
6. Coakley FV. Staging ovarian cancer: role of imaging. Radiol Clin North Am 2002;40(3):609-36.
7. Le Bihan D. Diffusion/perfusion MR imaging of the brain: from structure to function. Radiology 1990;177(2):328-29.
8. Yoshikawa T, Kawamitsu H, Mitchell DG, Ohno Y, Ku Y, Seo Y, et al. ADC measurement of abdominal organs and lesions using parallel imaging technique. AJR 2006;187(6):1521-30.
9. Funt SA, Hann LE. Detection and characterization of adnexal masses. Radiol Clin North Am 2002;40(3):591-608.
10. Fleischer AC, Daniell JF, Rodier J, Lindsay AM, James AE Jr. Sonographic monitoring of ovarian follicular development. J Clin Ultrasound 1981;9(6):275-80.
11. Togashi K. MR imaging of the ovaries: normal appearance and benign disease. Radiol Clin North Am 2003;41(4):799-811.
12. Outwater EK, Mitchell DG. Normal ovaries and functional cysts: MR appearance. Radiology 1996;198(2):397-402.
13. Russell DJ. Adnexal mass: detection and evaluation. In: Fleischer AC, Javitt MC, Jeffrey RB, Jones HW, eds. Clinical Gynecologic Imaging. 1st ed. Philadelphia: Lippincott-Raven; 1997. p. 43-106.
14. Moteki T, Ishizaka H. Diffusion-weighted EPI of cystic ovarian lesions: evaluation of cystic contents using apparent diffusion coefficients. J Magn Reson Imaging 2000;12(6):1014-9.
15. Nakayama T, Yoshimitsu K, Irie H, Aibe H, Tajima T, Nishie A, et al. Diffusion-weighted echoplanar MR imaging and ADC mapping in the differential diagnosis of ovarian cystic masses: usefulness of detecting keratinoid substances in mature cystic teratomas. J Magn Reson Imaging 2005;22(2):271-8.
16. Katayama M, Masui T, Kobayashi S, Ito T, Sakahara H, Nozaki A, et al. Diffusion-weighted echo planar imaging of ovarian tumors: is it useful to measure apparent diffusion coefficients? J Comput Assist Tomogr 2000;26(2):250-6.
17. Takeuchi M, Matsuzaki K, Nishitani HJ. Diffusion-weighted magnetic resonance imaging of ovarian tumors: differentiation of benign and malignant solid components of ovarian masses. J Comput Assist Tomogr 2010;34(2):173-6.
18. Kilickesmez O, Bayramoglu S, Inci E, Cimilli T, Kayhan A. Quantitative diffusion-weighted magnetic resonance imaging of normal and diseased uterine zones. Acta Radiol 2009;50(3):340-7.
19. Fujii S, Matsusue E, Kanasaki Y, Kanamori Y, Nakanishi J, Sugihara S, et al. Detection of peritoneal dissemination in gynecological malignancy: evaluation by diffusion-weighted MR imaging. Eur Radiol 2007;18(1):18-23.